

Fault-Tolerant Control using Adaptive Time-Frequency Method in Bearing Fault Detection for DFIG Wind Energy System

Suratsavadee Koonlaboon KORKUA

School of Engineering and Resources, Walailak University, Nakhon Si Thammarat 80161, Thailand

(Corresponding author's e-mail: ksuratsa@wu.ac.th)

Received: 22 March 2013, Revised: 15 November 2013, Accepted: 15 January 2014

Abstract

With the advances in power electronic technology, doubly-fed induction generators (DFIG) have increasingly drawn the interest of the wind turbine industry. To ensure the reliable operation and power quality of wind power systems, the fault-tolerant control for DFIG is studied in this paper. The fault-tolerant controller is designed to maintain an acceptable level of performance during bearing fault conditions. Based on measured motor current data, an adaptive statistical time-frequency method is then used to detect the fault occurrence in the system; the controller then compensates for faulty conditions. The feature vectors, including frequency components located in the neighborhood of the characteristic fault frequencies, are first extracted and then used to estimate the next sampling stator side current, in order to better perform the current control. Early fault detection, isolation and successful reconfiguration would be very beneficial in a wind energy conversion system. The feasibility of this fault-tolerant controller has been proven by means of mathematical modeling and digital simulation based on Matlab/Simulink. The simulation results of the generator output show the effectiveness of the proposed fault-tolerant controller.

Keywords: Doubly-fed induction generator (DFIG), fault-tolerant control, monitoring, wind turbine, rotor side inverter, bearing fault

Introduction

Growing towards a major energy source, the wind energy industry has developed rapidly throughout the last 10 - 20 years [1]. The generated wind energy depends on the wind potential and the turbine availability, and is impacted by faults and repairs. It is crucial to ensure the reliable operation of wind power systems in order to improve both the quantity and quality of wind power generation. Therefore, supervisory control and data acquisition (SCADA) systems record wind turbine parameters, which can be used to monitor their performance. Data envelopment analysis (DEA), which is an analytical technique to assess the capacity of wind turbines, is applied to identify the critical faults in wind turbines [2].

Before exploring condition monitoring and fault diagnostic methods in wind turbines, the different kinds of failures are reviewed [3-7]. Bearing faults account for over 40 % of all machine faults [8]. They develop through the years in the industrial process from degrading bearing surfaces. Consequently, many bearing fault detection techniques in the literature are reviewed [9-13]. However, those techniques are applied mainly in order to detect and monitor the machine behaviors; given those detections, the fault indicators can be achieved.

In order to improve the quality of wind turbine output by integrating the bearing fault detection scheme in the control system, this paper studies fault-tolerant controls. Fault-tolerant controllers are designed to maintain an acceptable level of performance in mechanical fault conditions. The main objective in this designed fault-tolerant control is to apply bearing fault detection techniques, based on measured motor current data, to detect the fault occurrence in the system, and then let the controller

compensate for faulty conditions. Early fault detection, isolation and successful reconfiguration would be very beneficial in wind energy conversion systems. The doubly-fed induction generator (DFIG) wind turbine control system is studied, and a fault-tolerant control strategy for the rotor side inverter controller, to suppress the power fluctuation due to bearing faults, is also proposed. In this research, an adaptive statistical time-frequency method is used for bearing fault detection. The feature vectors, including frequency components located in the neighborhood of the characteristic fault frequencies, is first extracted, and then used to estimate the next sampling stator side current, in order to better perform the current control. Modification of decoupling voltage control makes it possible to obtain the estimated rotor voltage that is needed to inject the desired current into the DFIG, via the current-controlled voltage source PWM inverter. The feasibility of this design has been proven by means of mathematical modeling and digital simulation based on Matlab/Simulink. The simulation results of the generator output show the effectiveness of the proposed fault-tolerant controller.

Materials and methods

Fault-tolerant design is a design that enables a system to continue operation, possibly at a reduced level (also known as graceful degradation), when some part of the system fails, rather than failing completely. It is determined by the ability of the control system to maintain the control objectives, despite the occurrence of a fault [14]. Dynamic systems, such as wind energy systems, can be subjected to various faults, caused by actuator, sensor, or component failures. Once a fault happens, it can occur both at the component level and in the overall system. Fault propagation in the overall control system, composed of 6 sub-systems, can be shown in **Figure 1**. One can see that a fault occurs in sub-system No. 2, propagates in the system, and influences all of the other sub-system/components.

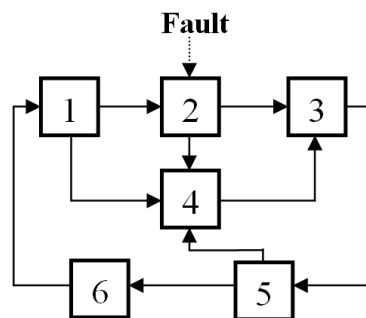


Figure 1 Fault propagation in the overall system.

The effects of a fault in a single component may be just a minor problem. However, due to fault propagation throughout the overall system, it may eventually cause system failure. It would be very beneficial if fault-tolerant control is applied to the design. In passive fault-tolerant control, a fixed controller is designed that tolerates changes of the plant dynamics. In active fault-tolerant control, a more advanced design, the controller parameters are adapted to the dynamic plant parameters. All of the important parameters are adjusted by a fault monitoring and detection scheme. The proposed control system, into which the fault monitoring and diagnosis are integrated, is shown in **Figure 2**. Once the bearing fault occurs, this control will be able to redesign by adapting the rotor-side controller parameters to the dynamic properties of the faulty system. The inputs and outputs of the wind turbine system used in the control loop remain the same as for the initial design (a faultless case).

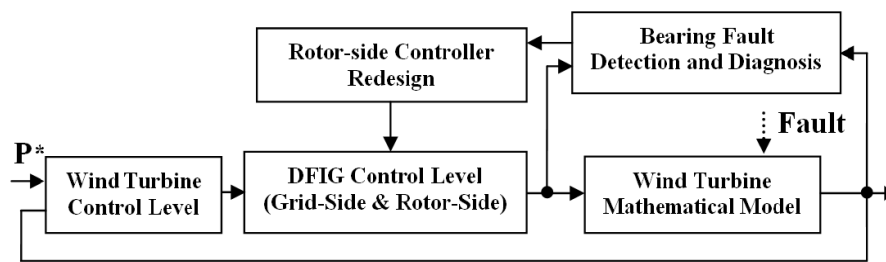


Figure 2 The block diagram of the proposed control System with bearing fault detection and diagnostic algorithm.

Wind turbine monitoring and fault diagnosis

Analysis of wind farm maintenance costs has shown that up to 40 % of the cost can be related to unexpected failures of components that lead to unscheduled corrective maintenance actions [4,5]. Reference [6] shows the annual average downtimes of major wind turbine subassemblies, according to a LWK survey of more than 2,000 wind turbines over 11 years. It is seen that the gearbox is ranked as the most critical of subassemblies; consequently, they should received the highest priority for monitoring, due to the high downtime caused by their malfunction.

Condition based monitoring is used primarily to detect faults in mechanical components, such as the bearings and gears installed inside a wind turbine nacelle. Therefore, in this work, we mainly focus on the bearing fault monitoring of wind turbines. The goal for this research is not only to monitor the machine health of wind turbine system, but also to develop a fault-tolerant control method for doubly-fed induction generators (DFIG) that addresses the issues associated to the bearing fault condition of the generator.

Characteristics of bearing fault frequencies

According to well-documented reports, motor current signature analysis (MCSA) has received more and more attention in fault detection research [15-17]. It has been well established that the characteristics of bearing fault frequencies in vibration can be reflected into stator current. Since the characteristic bearing fault frequencies are a good indicator of defects, virtually all current techniques to detect defects are based on indentifying and processing those fault frequencies in the stator current. When a fault in one surface of a rolling element bearing strikes another surface, it produces an impulse, which may excite resonances in the bearing and in the machine. As the bearing rotates, these impulses will appear periodically with a frequency which is determined uniquely by the location of the fault, maybe on the inner ring, outer ring, or one of the rolling elements (ball). The cross-sectional view of a bearing and the geometric parameters can be seen in **Figure 3**.

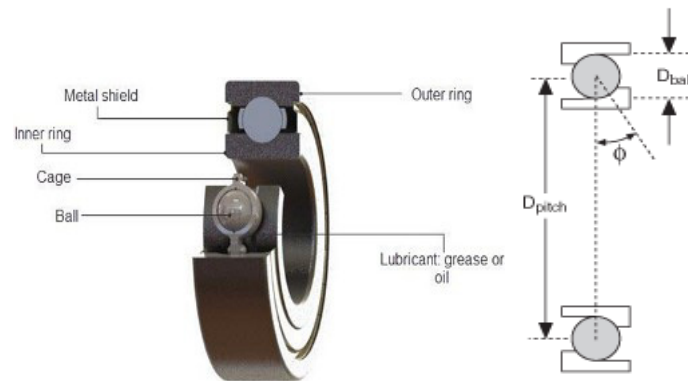


Figure 3 Cross-sectional view of bearing with geometric parameters.

Therefore, the shift from healthy to faulty bearing conditions would cause changes in the bearing vibration signals. This can be predicted from the bearing geometry and the speeds at which the machine rotates. The relationship between the vibration frequencies for bearing faults can be reflected into stator current, and can be described as [18];

Characteristic frequency of the outer ring fault of the bearing:

$$f_c = \frac{f_s}{2} \left[1 - \frac{D_B}{D_P} \cos \phi \right] \quad (1)$$

Characteristic frequency of the inner ring fault of the bearing:

$$f_c = \frac{f_s}{2} \left[1 + \frac{D_B}{D_P} \cos \phi \right] \quad (2)$$

Characteristic frequency of the rolling element fault:

$$f_c = \frac{D_P}{2D_B} f_s \left[1 - \left(\frac{D_B}{D_P} \right)^2 \cos^2 \phi \right] \quad (3)$$

where f_s is the shaft rotating frequency in Hertz, D_P is the diameter of the bearing pitch, D_B is the diameter of the ball, and ϕ is the contact angle.

Current signature extraction

In this research, an adaptive statistical time-frequency method proposed by Yazici and Kliman is used for bearing fault detection [19]. This technique is performed and applied to verify the effectiveness of bearing fault detection in this work. A schematic diagram is illustrated in **Figure 4**. This technique treats stator current as a non-stationary signal. First, a time frequency spectrum is estimated after preprocessing, and feature vectors are extracted from the spectrum. In this research, the feature vectors, including frequency components located in the neighborhood of the characteristic fault frequencies (along the frequency axis). Next, the feature space is segmented into different normal conditions of the machine. These resulting segments are grouped as a mode, and then a representative and a threshold are determined.

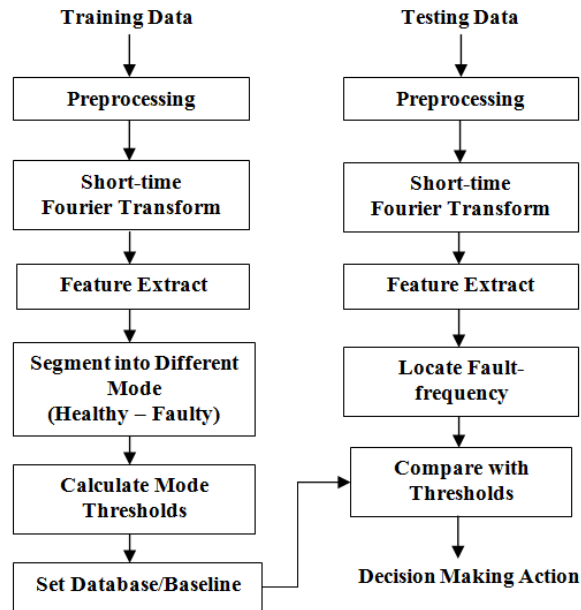


Figure 4 Schematic diagram of current monitoring technique based on time-frequency transform.

Once the algorithm is trained for all normal operating conditions, a data base, or baseline, is then calculated. For testing data, after the same preprocessing, short time Fourier transform and feature extraction, the feature vector is then calculated and located on the frequency axis. In this work, only 2 modes, healthy mode and faulty mode, are classified.

Operation of wind generation system

The overall control structure of the wind turbine system consists of an aerodynamic model, a transmission system, a generator model, a DFIG control level block model, and a wind turbine control level block model [20]. As shown in **Figure 5**, the stator of the DFIG is connected directly to the incoming AC mains, whereas the wound rotor is fed from the power electronics converter through slip rings. A wind turbine control level provides reference signals both to the pitch system of the wind turbine and to the DFIG control level. It contains 2 controllers: a Power Controller and a Pitch Controller. It generates an active power reference signal for the active power control loop, performed by the rotor side inverter controller in the DFIG control level. A DFIG control level contains the electrical control of the power converters and of the doubly-fed induction generator with a fast dynamic response. It contains 2 controllers: a Grid side converter controller and a Rotor side inverter controller.

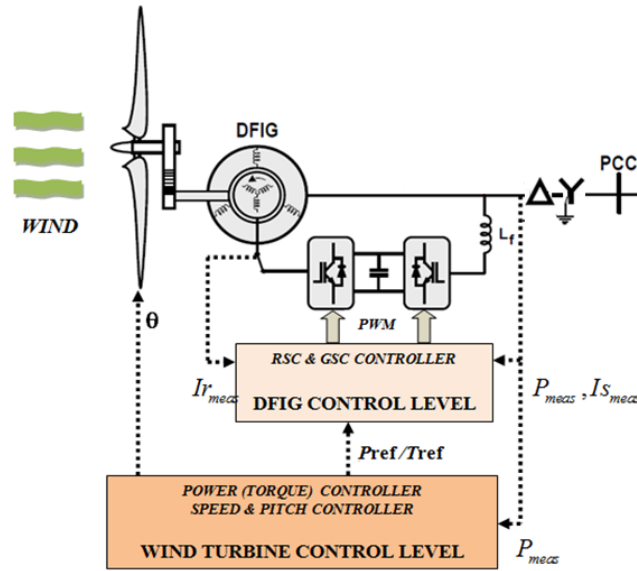


Figure 5 Configuration of a DFIG wind turbine.

Using Park's transformation from a stationary (a-b-c) reference frame to a rotating (d-q) reference frame, the dynamic model for a wound rotor induction machine (DFIG) is defined as follows [21]:

Stator voltage equations on a d-q reference frame;

$$\begin{aligned} V_{sd} &= p\lambda_{sd} - \omega\lambda_{sq} + R_s i_{sd} \\ V_{sq} &= p\lambda_{sq} + \omega\lambda_{sd} + R_s i_{sq} \end{aligned} \quad (4)$$

Rotor voltage equations on a d-q reference frame;

$$\begin{aligned} V_{rd} &= p\lambda_{rd} - (\omega - \omega_r)\lambda_{rq} + R_r i_{rd} \\ V_{rq} &= p\lambda_{rq} + (\omega - \omega_r)\lambda_{rd} + R_r i_{rq} \end{aligned} \quad (5)$$

Stator flux equations on a d-q reference frame;

$$\begin{aligned} \lambda_{sd} &= (L_{ls} + L_m)i_{sd} + L_m i_{rd} \\ \lambda_{sq} &= (L_{ls} + L_m)i_{sq} + L_m i_{rq} \end{aligned} \quad (6)$$

Rotor flux equations on a d-q reference frame;

$$\begin{aligned}\lambda_{rd} &= (L_{lr} + L_m)i_{rd} + L_m i_{sd} \\ \lambda_{rq} &= (L_{lr} + L_m)i_{rq} + L_m i_{sq}\end{aligned}\quad (7)$$

The electromagnetic torque, the power, and the reactive power equations may be written as;

$$\begin{aligned}T_s &= -\frac{3}{2}p(\lambda_{sd}i_{sq} - \lambda_{sq}i_{sd}) \\ P_s &= \frac{3}{2}(V_{sd}i_{sd} + V_{sq}i_{sq}) \\ Q_s &= \frac{3}{2}(V_{sq}i_{sd} - V_{sd}i_{sq})\end{aligned}\quad (8)$$

where L and R are the inductance and resistance, respectively.

The proposed fault-tolerant controller

The proposed method intends to design a fault-tolerant control strategy on the rotor side inverter to help reduce the oscillation of the wind output when bearing fault affects the generator. The current control approach, considering a vector oriented control (VOC) philosophy in the d-q reference frame, is applied. The rotor side inverter independently controls the active and reactive power. The power is controlled indirectly by controlling the rotor current. In this control scheme, the rotor side inverter is controlled in a synchronously rotating d-q axis reference frame, with the d-axis oriented along the stator-flux vector position. Under a power-speed control, combining the stator flux amplitude/phase angle estimator with feature current vector extraction, the current components at the oscillating frequency are extracted. This rotor current is also used to estimate the next sampling stator side current, in order to better perform the current control. Modification of the decoupling voltage control makes it possible to obtain the estimated rotor voltage that is needed to inject the desired current into the DFIG via the current-controlled voltage source PWM inverter.

Stator flux magnitude and phase angle estimation

From the coordinate of the stator flux on the d-q reference frame, the expression of the stator flux magnitude ($|\lambda_s|$) can be defined as;

$$\begin{aligned}\lambda_{sd} &= \int (V_{sd} - R_s i_{sd}) dt \\ \lambda_{sq} &= \int (V_{sq} - R_s i_{sq}) dt \\ |\lambda_s| &= \sqrt{(\lambda_{sd})^2 + (\lambda_{sq})^2}\end{aligned}\quad (9)$$

The phase angle (θ_e) is calculated by;

$$\theta_e = \tan^{-1} \frac{\lambda_{sq}}{\lambda_{sd}}\quad (10)$$

Stator side current estimation

The objective of this part will be focused on finding a relationship between the state space variables that could permit prediction of the behavior of the DFIG under faulty conditions. The predicted output response of the stator current should be closed to the real stator current and should have a fast dynamic response. First, considering that the dynamic voltage equation of the rotor is linear, and assuming that the magnetic circuit of DFIG is linear, by applying the Laplace transformation, we can obtain the stator current on the d-q rotating frame as follows;

$$\begin{aligned}
 i_{sd} &= \frac{(L_s s + R_s)V_{sd} + \omega_s L_s V_{sq}}{L_s^2 s^2 + 2L_s R_s s + R_s^2 + \omega_s^2 L_s^2} - \frac{(L_s s^2 + R_s s + \omega_s^2 L_s)L_m i_{rd} - R_s \omega_s L_m i_{rq}}{L_s^2 s^2 + 2L_s R_s s + R_s^2 + \omega_s^2 L_s^2} \\
 i_{sq} &= \frac{(L_s s + R_s)V_{qs} - \omega_s L_s V_{sd}}{L_s^2 s^2 + 2L_s R_s s + R_s^2 + \omega_s^2 L_s^2} - \frac{(L_s s^2 + R_s s + \omega_s^2 L_s)L_m i_{rq} + R_s \omega_s L_m i_{rd}}{L_s^2 s^2 + 2L_s R_s s + R_s^2 + \omega_s^2 L_s^2}
 \end{aligned}
 \tag{11}$$

By considering that the stator flux is aligned with the d-q reference frame, and hence its quadrature component is zero. Assuming that the leakage inductance is low, and the inductive reactance is much greater than the stator resistance, it can be concluded that the stator's voltage term tends to zero. This equation can be reduced, and the predicted stator current on d-q component ($\hat{i}_{sd}, \hat{i}_{sq}$) can be as shown below;

$$\begin{aligned}
 \hat{i}_{sd} &= \frac{1}{\omega_s L_s} V_{sq} - \frac{L_m}{L_s} i_{rd} \\
 \hat{i}_{sq} &= -\frac{L_m}{L_s} i_{rq}
 \end{aligned}
 \tag{12}$$

Modified decoupling voltage control

The aim of this analysis is to control the d-q current components used in the rotor side inverter. Using a stator flux-oriented approach, implementation with the current-controlled PWM converter requires a decoupling control scheme [22]. Substituting this leakage factor equation into the rotor flux equations, and rearranging the d-q rotor voltage equations, we obtain the following;

$$\begin{aligned}
 V_{rd} &= R_r i_{rd} + \sigma L_r \frac{di_{rd}}{dt} - \omega_{slip} \sigma L_r i_{rq} \\
 V_{rq} &= R_r i_{rq} + \sigma L_r \frac{di_{rq}}{dt} + \omega_{slip} (\sigma L_m i_{ms} + \sigma L_r i_{rd})
 \end{aligned}
 \tag{13}$$

The current errors on both d-q components are processed by the PI controller to give V'_{rd} , and V'_{rq} respectively. This voltage output can be formed as follow;

$$\begin{aligned}
 V'_{rd} &= R_r i_{rd} + \sigma L_r \frac{di_{rd}}{dt} \\
 V'_{rq} &= R_r i_{rq} + \sigma L_r \frac{di_{rq}}{dt}
 \end{aligned}
 \tag{14}$$

To ensure good tracking of the current control, with a fast dynamic response, the above decoupling voltage equations need to be modified. All compensation terms are added to the reference voltages, making it possible to achieve the decoupled performance of the stator flux-oriented control of the rotor side inverter controller, also taking into account the predicted stator current. In order to eliminate the harmonics of the current components at the oscillating frequency i_{rd_osc} , the compensation voltage, calculated from oscillating current extraction, will be added. Finally, the modified reference voltages command can be represented as in these following equations;

$$\begin{aligned}
 V_{rd}^* &= V'_{rd} + i_{rd}^* R_r - \omega_{slip} (L_r i_{rd}^* + L_m \hat{i}_{sd}) + i_{rd_osc} R_r \\
 V_{rq}^* &= V'_{rq} + i_{rq}^* R_r + \omega_{slip} (L_r i_{rq}^* + L_m \hat{i}_{sq}) + i_{rd_osc} \omega_{slip} L_r
 \end{aligned}
 \tag{15}$$

Results and discussion

The proposed control of the rotor side inverter was verified on a 9MW wind farm with a GE1.5MW doubly fed induction generator (DFIG) through a computer simulation. It was assumed that the DFIGs in the wind farm acted coherently. All machine parameters and aerodynamic characteristics of this device are presented in **Table 1**.

Table 1 9-MW wind farm parameters in this study.

Parameter (Unit)	Value
Nominal power (MVA)	9
Rated voltage (V)	575
Nominal frequency(Hz)	60
Stator resistance (p.u.)	0.023
Stator leakage inductance (p.u.)	0.18
Magnetizing inductance (p.u.)	2.9
Rotor resistance (p.u.)	0.016
Rotor leakage inductance (p.u.)	0.16
Number of pairs of poles	2
Nominal DC voltage (V)	1200

The NTN rolling bearing parameters which are mostly used in 1.5MW wind turbines were used in this study. From the NTN part number datasheet 240/600 BK30D1, the following parameters were obtained. The outside diameter is 870 mm and the inside one is 600 mm. The ball diameter is 272 mm, with a contact angle of zero. The system performance and capabilities of the discussed fault tolerant control were tested under different conditions, carried out on MATLAB/Simulink. The main important events of real wind speed were used as the wind speed input; wind was ramped up and ramped down, to

perform tests under both healthy and faulty conditions. The simulation was done for a normal bearing and for 2 defective bearings, namely inner ring fault and outer ring fault. The generator speed was performed under maximum power point tracking, following the wind speed profile. According to the calculation formula of characteristic frequency of the bearing fault at different generator speeds, the fault feature frequency of bearing parts was also at a time-varying fault frequency.

As the first step in the simulation, the motor current signal was fed into the machine analysis to identify the important features extracted. Based on the adaptive statistical analysis, the spectrum amplitude in the expected rotational frequency range was successfully extracted. The Fast Fourier Transform (FFT) algorithm was used to perform discrete Fourier transformations (DFTs) for all current signals. In order to keep all other frequency current components, the frequency-varying band-pass filter was used to extract only the oscillating current component at a particular frequency. This came to effect only in the presence of the fault. It was designed to have a large gain at the known disturbance frequency (oscillating frequency), but also have a negligible effect at all other frequencies. This current extraction was successfully done by using a high-Q second order band-pass filter.

It was noteworthy that the machine current data were obtained from a wind turbine emulator in the Matlab simulation, incorporating the properties of both natural wind and the turbine rotor aerodynamic behavior. Although the level of fault simulated was not performed in an experimental test bed, which would provide a noise-rich environment, the demonstrated performance was still promising for practical applications and robustness.

Wind ramp up with inner ring fault

To perform the proposed control capability during wind ramp up, the inner ring fault was applied into the system at $t = 3$ seconds, and later the fault tolerant controller was introduced at $t = 6$ seconds. The simulation results, depicted in **Figure 6**, show the response of the wind speed, generated output power and torque during the wind ramp up event. When the inner ring fault occurred at $t = 6$ second, the power output and torque started to oscillate, which can be seen from zoomed version results. The oscillating frequency varied due to the wind speed. **Figure 7** illustrates the wind generator behavior both before and after the fault scenarios. The stator current fed back to the grid finally reverted back to a sinusoidal waveform. The simulation results confirmed the effectiveness of the proposed control scheme during the wind ramp up case.

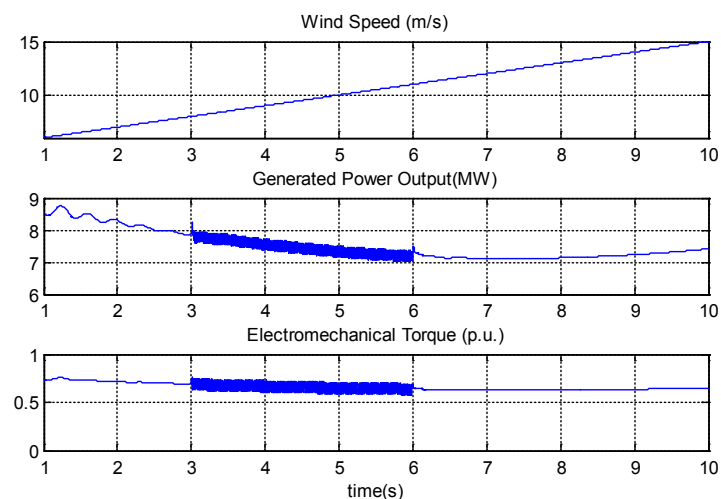


Figure 6 Simulation results of DFIG outputs: Wind Speed (m/s), Power Output (MW), Torque (p.u.) obtained on Wind Ramp Up with inner ring fault.

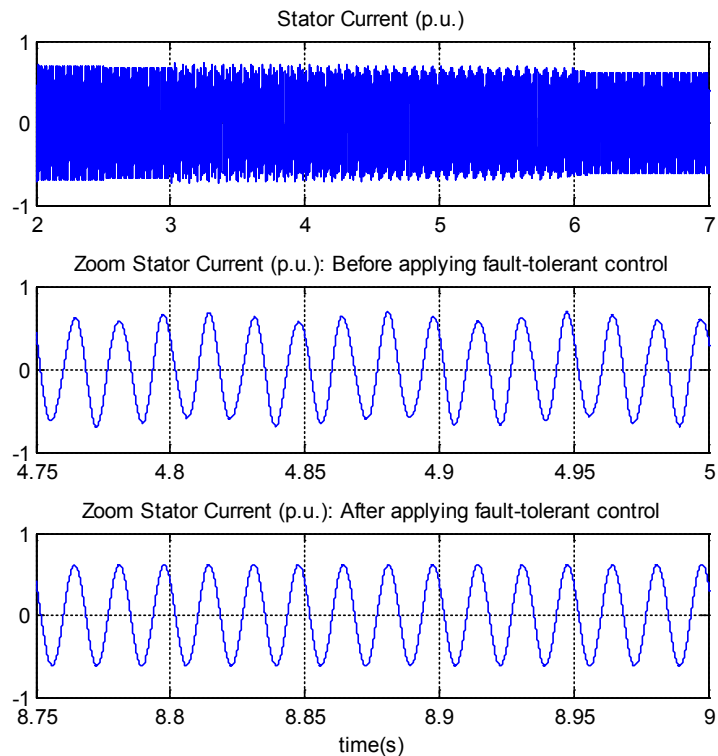


Figure 7 Simulation Results of Generated Current Output (p.u.) and Zoomed versions of current output.

Wind ramp down with outer ring fault

The simulation results, depicted in **Figure 8**, show the response of the wind speed, generator speed, generated output power and torque during the wind ramp down event. When the outer ring fault occurred at $t = 3$ seconds, the power output and torque started to oscillate, which can be seen from the zoomed version results in **Figure 9**. The oscillating frequency varied due to the wind speed. After $t = 6$ seconds, in **Figure 9**, the stator current fed back to the grid finally reverted back to a sinusoidal waveform. One can see from the simulation results that the proposed control scheme also operated properly during the wind ramp down event.

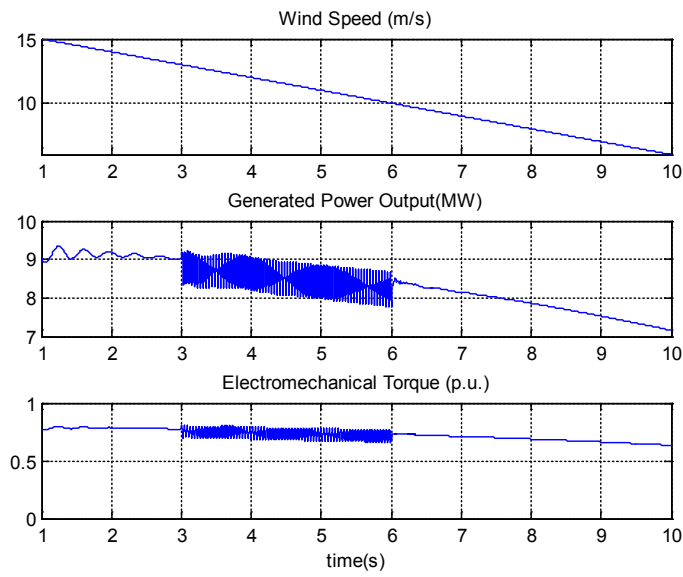


Figure 8 Simulation results of DFIG outputs: Wind Speed (m/s), Power Output (MW), Torque (p.u.) obtained on Wind Ramp Down with outer ring fault.

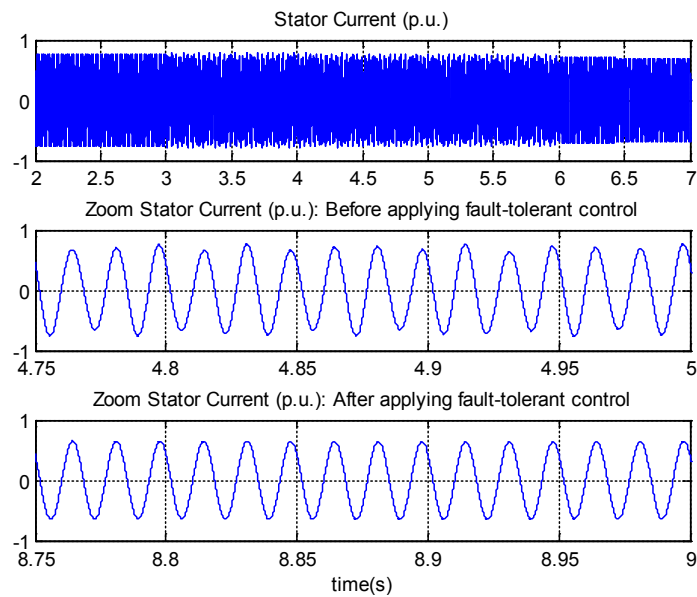


Figure 9 Simulation Results of Generated Current Output (p.u.) and Zoomed versions of current output.

Conclusions

This paper presents an experiment into fault tolerance control of a DFIG wind turbine. The results show that the DFIG is able to extract the maximum power by tracking the power speed characteristic. When a bearing fault occurs in the wind turbine system, the output signals, such as power, torque, and current, will oscillate at the bearing fault frequency, under the traditional control scheme. This can be seen directly from the simulation results. Once the fault tolerant control is introduced into the wind energy system, the oscillation of the power and current waveform is significantly improved. At the steady state response region, DFIG can recover back to normal operation, where the stator current reverts back to a sinusoidal waveform. The power output waveform show less ripple. Additionally, an adaptive statistical time-frequency method is used for bearing fault detection in both inner and outer ring fault. The feature vectors, including frequency components located in the neighborhood of the characteristic fault frequencies, is successfully extracted, and then used to estimate the next sampling stator side current, in order to better perform the current control. The simulation results show the effectiveness of this proposed fault tolerance control, based on the rotor side inverter controller.

References

- [1] WL Kling and JG Sloopweg. Wind turbines as power plants. *In: Proceedings of the IEEE Cigré Workshop on Wind Power and the Impacts on Power Systems*, Oslo, Norway, 2002.
- [2] A Kusiak, A Verma and X Wei. Wind Turbine Frontier from SCADA. *Wind Syst. Mag.* 2012; **3**, 36-9.
- [3] T Burton, D Sharpe, N Jenkins and E Bossanyi. *Wind Energy Handbook*. John Wiley & Sons, 2001.
- [4] M Wilkinson, F Spianto, M Knowles and PJ Tavner. Towards the zero maintenance wind turbine. *In: Proceedings of the 41st International Universities Power Engineering Conference*, Newcastle-upon-Tyne, 2006, p. 74-8.
- [5] D McMillan and GW Ault. Quantification of condition monitoring benefit for offshore wind turbines. *Wind Eng.* 2007; **31**, 267-85.
- [6] PJ Tavner, GJW van Bussel and F Spinato. Machine and converter reliabilities in wind turbines. *In: Proceedings of the 3rd IET International Conference on Power Electronics, Machines and Drives*, Dublin, Ireland, 2006, p. 127-30.
- [7] P Caselitz and J Giebhardt. *Advanced Maintenance and Repair for Offshore Wind Farms using Fault Prediction and Condition Monitoring Techniques (OffshoreM&R)*. The European Commission, DG TREN.
- [8] IAS Motor Reliability Working Group. Report of large motor reliability survey of industrial and commercial installations: Part I and Part II. *IEEE Trans. Ind. Appl.* 1985; **21**, 853-72.
- [9] JR Stack, TG Habetler and RG Harley. Fault classification and fault signature production for rolling element bearings in electric machines. *IEEE Trans. Ind. Appl.* 2004; **40**, 735-9.
- [10] RR Schoen, TG Habetler, F Kamran and RG Bartheld. Motor bearing damage detection using stator current monitoring. *IEEE Trans. Ind. Appl.* 1995; **31**, 1274-9.
- [11] M Blodt, P Granjon, B Raiso and G Rostaing. Models for bearing damage detection in induction motors using stator current monitoring. *IEEE Int. Symp. Ind. Electron.* 2004; **1**, 383-8.
- [12] JR Stack, TG Habetler and RG Harley. Bearing fault detection via autoregressive stator current modeling. *IEEE Trans. Ind. Appl.* 2004; **40**, 740-7.
- [13] Y Amirat, V Choqueuse, MEH Benbouzid and JF Charpentier. Bearing fault detection in DFIG-based wind turbines using intrinsic mode function. *In: Proceedings of the XIX International Conference on Electrical Machines*, Rome, Italy, 2010.
- [14] S Pourmohammad and A Fekih. Fault-Tolerant control of wind turbine systems-A review. *In: Proceedings of the IEEE Green Technologies Conference*, Baton Rouge, LA, 2011.
- [15] MEH Benbouzid, M Vieira and C Theys. Induction motors' faults detection and localization using stator current advanced signal processing techniques. *IEEE Trans. Power Electron.* 1999; **14**, 14-22.

- [16] WJ Wiedenbrug, A Ramme, E Matheson, VA Jouanne and AK Wallace. Modern online testing of induction motors for predictive maintenance and monitoring. *IEEE Trans. Ind. Appl.* 2002; **38**, 1466-72.
- [17] A Bellini, F Filippetti, G Franceschini, C Tassoni, R Passaglia, M Saottini, G Tontini, M Giovannini and A Rossi. On-field experience with online diagnosis of large induction motors cage failures using MCSA. *IEEE Trans. Ind. Appl.* 2002; **38**, 1045-53.
- [18] SA McInerny and Y Dai. Bearing vibration signal processing for bearing fault detection. *IEEE Trans. Educ.* 2003; **46**, 149-56.
- [19] W Zhou, TG Habetler and RG Harley. Stator current-based bearing fault detection techniques: A general review. *In: Proceedings of the IEEE International Symposium on Diagnostics for Electric Machines, Power Electronics and Drives, Cracow, 2007.*
- [20] LH Hansen, L Helle, F Blaabjerg, E Ritchie, S Munk-Nielsen, H Bindner, P Sørensen and B Bak-Jensen. *Conceptual Survey of Generators and Power Electronics for Wind Turbines.* Risø National Laboratory, Roskilde, Denmark, 2001.
- [21] P Krause, O Wasynczuk and S Sudhoff. *Analysis of Electric Machinery and Drive Systems.* 2nd ed. New York, IEEE Press, 2002.
- [22] R Pena, JC Clare and GM Asher. Doubly fed induction generator using back-to-back PWM converters and its application to variable speed wind-energy generation. *IEEE Proc. Electron. Power Appl.* 1996; **143**, 231-41.